Biological and Biomedical Journal

Journal homepage: https://bbj.journals.ekb.eg

Biomedical applications of eco-friendly myco-synthesized zinc oxide nanoparticles using *Penicillium citrinum* Mekky2025

Ahmed M. Baiomy[1], Husein H. El-Sheikh[2], Mohammed H. Mourad[1], Alsayed E. Mekky[2,*]

[1]The Regional Center for Mycology and Biotechnology, Al-Azhar University, Cairo, Egypt

[2] Botany and Microbiology Department, Faculty of Science, Al-Azhar University, Cairo, Egypt

ARTICLE INFO

Received: 15/1/2025
Revised: 30/5/2025
Accepted: 15/6/2025

Corresponding author:
Alsayed E. Mekky, Ph. D
E-mail: alsayedessam@azhar.edu.eg
Mobile: (+2)01222806275

P-ISSN: 2974-4334
E-ISSN: 2974-4342
DOI:
10.21608/BBJ.2025.353427.1074

ABSTRACT

The biological synthesis of metal oxide nanoparticles using fungi presents a sustainable and eco-friendly alternative to conventional methods. In this study, *Penicillium citrinum* FN.6 was isolated from soil and identified through both traditional and molecular techniques. Gas chromatography-mass spectrometry (GC-MS) analysis of the fungal extract (PCE) revealed the presence of various bioactive compounds, predominantly 9,12-octadecadienoic acid (Z,Z)- and n-hexadecanoic acid. The extract was used to successfully synthesize zinc oxide nanoparticles (ZnO-NPs). Characterization of the synthesized ZnO-NPs was conducted using UV–visible spectroscopy (showing a surface plasmon resonance peak at 363 nm), X-ray diffraction (XRD), transmission electron microscopy (TEM), and Fourier-transform infrared spectroscopy (FTIR). The ZnO-NPs exhibited a spherical shape with an average diameter of 85 ± 4.6 nm. Biological evaluation showed that ZnO-NPs had potent antifungal activity against *Candida albicans*, as confirmed by SEM and TEM analyses. Antioxidant activity assessed via the DPPH assay indicated a strong scavenging ability, with an IC_{50} value of 5.41 ± 0.3 µg/mL. Furthermore, the nanoparticles demonstrated notable hemolytic effect through membrane stabilization and displayed minimal cytotoxicity on normal cells with a CC_{50} of 18.2 ± 0.7 µg/mL. These findings suggest that *P. citrinum*-mediated ZnO-NPs possess promising biomedical potential due to their antioxidant, hemolytic, and antifungal properties, coupled with low toxicity to healthy cells.

Keywords: Antifungal, *Candida albicans*, Electron microscopy Nanotechnology, *Penicillium citrinum*, Toxicity

1. Introduction

Nanotechnology is a cutting-edge field that affects every single component of the lives of people (Mohanpuria et al., 2008; Liu et al., 2011). Nanoparticles (NPs) have been employed in several disciplines, including nanomedicine, where they receive a lot of attention (Jain, 2007). The most important biomedical agents are thought to be metallic NPs. Several scientists have created a variety of expensive physical and chemical procedures to achieve such geometries, including the use of hazardous substances that cause various biological threats (Moghaddam et al., 2015). It is necessary to develop eco-friendly processes through environmentally conscious synthesis and other biological techniques (Carrouel et al., 2020). Microorganisms may be employed in nanoparticle synthesis. Because of their capacity for metal bioaccumulation and tolerance, fungi have garnered increased interest in the study of biological synthesis of metallic NPs (Wiesmann et al., 2020). One distinct benefit of using fungi in the production of NPs is their ease of scale-up. Large-scale enzyme production is possible because fungi are highly efficient extracellular enzyme secretors (Muhammad et al., 2019; Abozaid et al., 2024). Economic acceptability and ease of using biomass is an additional advantage for the use of

green techniques mediated by fungi to produce metallic NPs. Furthermore, many species develop quickly, making it easy to cultivate and maintain them in a lab setting (Hefny et al., 2019). Most fungi are capable of high intracellular metal absorption and wall-binding (Alavi and Nokhodchi, 2021). Through the process of biomimetic mineralization and internal or extracellular reduction of enzymes, fungi can create metal nanoparticles, meso, and tiny structures (Wang et al., 2017; Wojnarowicz et al., 2018). One of the metal oxide nanomaterials is zinc oxide nanoparticles (ZnO-NPs) which are desirable and adaptable inorganic compounds because of their distinct physical and chemical properties. Their molecular formula is ZnO, and they have a wide radiation absorption spectrum, strong photo-stability, high electrochemical linking coefficient, and good chemical durability (Prabha and Jajoo, 2021).

A wide range of economic and additive items, such as porcelain, concrete, plastics, glass, lotions, oils, glues, sealing compounds, pigments, power sources, ferrites, fireproofing substances, beauty products, and sun protection products, as well as foods as sources of zinc nutrients, have been produced and used to make ZnO-NPs (Sirelkhatim et al., 2015; Eixenberger et al., 2017). Because of their tiny dimensions, nano-sized ZnO particles exhibit strong antibacterial properties. After they enter the bacterial cell, they can stimulate various bactericidal mechanisms, such as the bacterial core or surface, produce reactive oxygen species (ROS), discharge Zn^{2+}, and can even be engulfed by cells (da Silva et al., 2019; Yusof et al., 2019; Maťátková et al., 2022). The goal of the research is to biosynthesize ZnO-NPs using isolated *Penicillium citrinum* and assess its cytotoxic effect on normal cells in order to ensure that it is harmless, as well as evaluate its antibacterial, antioxidant, and anti-inflammatory properties.

2. Materials and methods

Microbes' isolation and purification

Soil samples were collected from a depth of approximately 12 cm at the Menoufia site area (31°36'42.7"N, 29°45'8.8"E). Each 1 g of soil was suspended in 100 mL of sterile distilled water for further analysis. One milliliter (1 mL) of serially diluted soil suspensions, ranging from 10^{-1} to 10^{-6}, was plated onto Czapek-Dox Agar medium (Reza et al., 2024). To prevent the growth of bacteria, 0.5% chloramphenicol was added (Al-Zahrani and Al-Garni, 2023). Each particular dilution was examined on three different plate sets. Following that, the plates were kept at 28±2°C for seven days in a row, or until the colonies began to show. To determine the fungal species, hyphae tips or cell populations were re-inoculated onto new plates. The cleansed isolates have been studied physically and under a microscope. Only pure strains were cultivated on Czapex-Dox Agar medium bends and kept at -4°C according to Allawi et al. (2022). The most effective cultures were selected based on their ability to produce metal oxide nanoparticles after the purification of fungal isolates.

Characterization of the fungus using traditional and molecular methods

Following normal protocol, the selected fungal strain, FN.6, was initially identified classically through morphological and phenotypic examination (Correa et al., 2021). It was subsequently recognized molecularly through internal transcribed space (ITS) sequence analysis. The ITS gene was amplified and sequenced using primers for ITS1 (5` CTTGGTCATATAGAGGAAGTAA-3´) and ITS4 (5` TCCTGCGCTTATT GATATGC 3´) (White et al., 1990). The ITS gene sequences of those that had been uploaded in GenBank were compared using the ClustalX 1.8 tool (http://www.clustal.org/clustal2). Furthermore, the phylogenetic tree was constructed using the neighbor-joining technique (MEGA v6.1) scheme, and its veracity was evaluated using the bootstrap assessment at 1000 repeats (Jiang et al., 2024).

Preparation of the fungal extract

0.2 liters of methanol were added to 2.0 g of crushed dry fungus, homogenized and macerated for three consecutive days at the ambient temperature. Conventional extraction involved placing the extract in a sonicator set to 40°C for 60 min. The extract was then filtered and condensed through a rotatory extractor and a vacuum at 40°C (Aamer et al., 2024).

GC-mass analysis of the fungal extract

The chemical constituents of the fungus were ascertained using a Trace GC1310-ISQ mass scanner (Shimadu, Japan) and a direct terminal column TG-5MS (32 m x 0.27 mm x 0.27 m film thickness). The column oven's heat was first kept at 42° C, then raised by 5°C/min to 210°C and held there for 5 minutes. Lastly, it was raised to 295°C by 5°C/min and maintained there for 15 min. The needle and MS transition line heaters were kept at 270°C and 290°C, respectively, while helium was used as the carrier gas at a steady flow rate of 1.1 ml/min. A diluted portion of 1 µl was automatically administered utilizing the automatic sampler AS1300 in split configuration and a GC with a 6 min liquid interval. Full scan EI mass spectrum has been acquired at 70 eV ionization voltages over the 40–1000 m/z range. The ion source's heat was set at 230 °C. The individual constituents of the compounds were identified by contrasting the retention durations and mass spectrum of each component to those contained in the WILEY 07 and NIST 11.1 mass spectrum databases (Naveed et al., 2025).

Preparation of zinc oxide nanoparticles

The fungal strain FN.6 was put into 100 milliliters of Potato Dextrose broth media (PD) and left to thrive for five days at 26 ± 2°C. Following the time spent incubating, the implanted PD broth solution (Thermo-fisher, USA) was turned up at 10,000 rpm for five minutes in order to obtain the fungal biomass, and any leftover medium ingredient was rinsed off three times with deionized water. Then, 10 g of the captured fungal biomass was mixed with 100 mL of deionized water and left in the dark for 24 hours while moving constantly at 150 rpm. Zinc nitrate hexahydrate [Zn $(NO_3)_2.6H_2O$] was combined with the supernatant, a fungus biomass filtrate, to create ZnO-NPs using a biochemical catalyst. The mixture was subsequently spun up (Sumanth et al., 2020).

Characterization of biosynthesized ZnO nanoparticles

UV- spectroscopy

By measuring the absorbance at a wavelength between 200 and 600 nm, UV-Vis spectroscopy (Genway Inc., USA) was used to assess the intensity of the color that developed after combining fungal biomass filtrate with metal precursor. To find the maximal surface plasmon resonance, 2 mL of the synthesized solution was added to a quartz cuvette, and the absorbance was monitored periodically (Yuvakkumar et al., 2014).

Fourier transform infrared analysis

FT-IR (Thermo-fisher, USA) was used to examine the functional groups in the fungal biomass filtrate and compare them with the function groups in biosynthesized ZnO-NPs. Potassium bromide (KBr, ≥98.0%) was mixed with 10 mg of synthesized ZnO-NPs and crushed to form a disc. Wavenumbers 400–4000 Cm-1 were then used for analyzing the disc (Pragati et al., 2018).

X-ray diffraction analysis

The arrangement and development of the myco-synthesized ZnO-NPs were examined using the XRD method (DW-XRD-2660A, China) linked to Cu-Kα as an X-ray source (λ = 1.54 Å) at 40 KV and 30 mA. Within two Theta values, spanning from 10° to 80°, the X-ray scan was completed. XRD examination and Debye-Scherrer's equation were used to calculate the average crystallite size of ZnO-NPs (Shobha et al., 2019).

Transmission electron microscope examination

The morphology, size, and shape of the ZnO nanoparticles synthesized via fungal mediation were examined using a transmission electron microscope (JEOL JEM-1010, Japan). The ZnO-NPs were dispersed in Milli-Q water through ultrasonication, and a few drops of the suspension were carefully placed onto carbon-coated copper grids. Excess liquid was removed by gently touching the edge of the grid with filter paper and allowed to dry under ambient conditions before imaging (Anand et al., 2020). In the case of biological specimen embedding for ultrastructural analysis, fungal samples were fixed in 2.5% glutaraldehyde for 2 hours, followed by post-fixation with 2% osmium tetroxide. Dehydration was performed using a graded ethanol series, and staining was carried out with 1% uranyl acetate. The specimens were then embedded in resin. Ultrathin sections were obtained using an ultramicrotome (Leica,

Germany) and examined using a TEM (JEOL, Japan) (Teodori et al., 2000).

Scanning electron microscope examination

To examine the exterior of both normal and treated samples, SEM was employed. At the National Research Centre, fixed specimens were coated with gold, dehydrated in a series of ethyl alcohols, and then viewed with a SEM (JOEL, Japan) (Pesaresi et al., 2020).

Testing antimicrobial activity

The agar well diffusion method was employed to evaluate the antifungal activity of the fungal extract, biosynthesized ZnO-NPs, and the standard antifungal drug itraconazole. A volume of 100 µL from each sample was loaded into wells in the agar plates inoculated with the test organisms. Following the incubation period, the diameters of the inhibition zones were measured and compared with those produced by the reference drug. Serial dilutions of the effective dose were prepared and tested against a range of fungal strains (Sayed et al., 2022).

The antioxidant activity of ZnO-NPs and PCE

The antioxidant activities of the green myco-synthesized ZnO-NPs and the fungal extract (PCE) was evaluated using the DPPH radical scavenging assay. Serial concentrations (1000–1.95 µg/mL) of both ZnO-NPs and PCE were prepared by dispersing the samples in Milli-Q water. One milliliter of each sample was mixed with 400 µL of Tris-HCl buffer (50 mM, pH 7.5) and 1 mL of DPPH solution prepared in methanol. The mixture was vortexed and incubated in the dark at 36°C for 30 min under continuous agitation at 100 rpm. Another set of ascorbic acid (positive reference) tests were conducted using the same settings and amounts. Furthermore, the test was carried out using the same incubation settings as the negative control condition, which included DPPH and Tris-HCl buffer devoid of ascorbic acid and ZnO-NPs (Deleanu et al., 2024).

Hemolytic activities of ZnO-NPs and PCE

Preparation of erythrocyte suspension

Fresh venous blood (3 mL) was collected from healthy human volunteers into heparinized tubes to prevent clotting. The samples were centrifuged at 3000 rpm for 10 min at room temperature. The plasma was carefully removed, and the red blood cell (RBC) pellet was washed and resuspended in an equal volume of normal saline. The volume was measured and adjusted to a 40% (v/v) suspension using an isotonic phosphate-buffered saline (PBS, pH 7.4). The buffer was prepared by dissolving 0.2 g of NaH_2PO_4, 1.15 g of Na_2HPO_4, and 9.0 g of NaCl in 1 liter of distilled water. The erythrocyte suspension was freshly prepared for each experiment (Luna-Vázquez-Gómez et al.,2021). Ethical approval for the use of human samples was granted by the Faculty of Science Research Ethics Board (Approval No. FSR 15162552), and all procedures were carried out in accordance with institutional ethical guidelines.

Hemolysis test

The membrane stabilization method was employed to assess the anti-inflammatory potential of PCE and the biosynthesized ZnO nanoparticles (ZnO-NPs). Hypotonic solutions of PCE and ZnO-NPs at concentrations of 100, 200, 400, 600, 800, and 1000 µg/mL were prepared in distilled water. Isotonic solutions with the same concentrations were also prepared in PBS. Each sample (5 mL) was added in duplicate into centrifuge tubes. Control groups included: Negative control: 5 mL of distilled water; Positive control: 5 mL of indomethacin solution (200 µg/mL). 0.1 mL of erythrocyte suspension (40%) was added to each tube. The mixtures were incubated at 37°C for 1 hour and then centrifuged at 13,000 rpm for 3 min. The supernatants were collected, and the absorbance of released hemoglobin was recorded at 540 nm using a UV-Vis spectrophotometer (Spectronic, Milton Roy, USA). The percentage inhibition of hemolysis was calculated using the following equation (Mekky et al., 2024):

% Inhibition of hemolysis = 1-((OD2-OD1)/ (OD3-OD1)) *100

where OD1 represents the test sample's absorbance in an isotonic solution, OD2 represents the test sample's absorbance in a hypotonic solution, and OD3 represents the control sample's absorbance in a hypotonic solution.

Assessment of ZnO -NPs cytotoxic potential

The cytotoxic effect of the biosynthesized ZnO-NPs was evaluated on WI-38 normal human lung fibroblast cells using the MTT assay. The

samples were first dissolved in DMSO and applied to the cells at concentrations ranging from 1000 to 31.25 µg/mL. Following treatment, the cells were incubated for 24 hours at 35°C to allow sample interaction. Subsequently, the culture medium was replaced with fresh medium, and the cells were further incubated for 4 hours. Afterward, 100 µL of MTT solution (5 mg/mL) was added to each well, and the plates were incubated at 35°C for an additional 4 hours to allow formazan crystal formation. The amount of viable cells was determined by measuring the absorbance of the solubilized formazan product at 560 nm using an automated microplate reader (Tecan F50, USA). Cell morphology and viability were also observed under an inverted microscope equipped with a CCD camera (OMAX, USA) (Ayub et al., 2024).

Statistical analysis

The average readings of three distinct repeats were utilized to communicate the results of a quantitative analysis of the gathered data using Graph Pad Prism V5, USA. The Tukey test at $p < 0.05$ was used in conjunction with the *t*-test or ANOVA to evaluate the variation throughout variables and identify any significant differences.

3. Results

Isolation and identification for producing fungus

Different fungal isolates (6) were obtained from the soil samples which were purified and tested for producing the ZnO-NPs. It could be noticed that the fungus with the code of (FN.6) was the most promising fungus in NPs production. It was terverticillate with smooth conidia with about 3.5 µm long. The conidiophore: length was 200-300 µm, metula: was 13-14 µm and phialides was 6 -13 µm long as shown in (Fig. 1A). The fungal species was genetically identified as *P. citrinum* and with the accession number PQ857194. with 99.40% similarity with gene bank isolates. Furthermore, its phylogenetic tree could be seen in (Fig.1B).

Fig. 1A. Microscopic examination for *P. citrinum* (Magnification=40X)

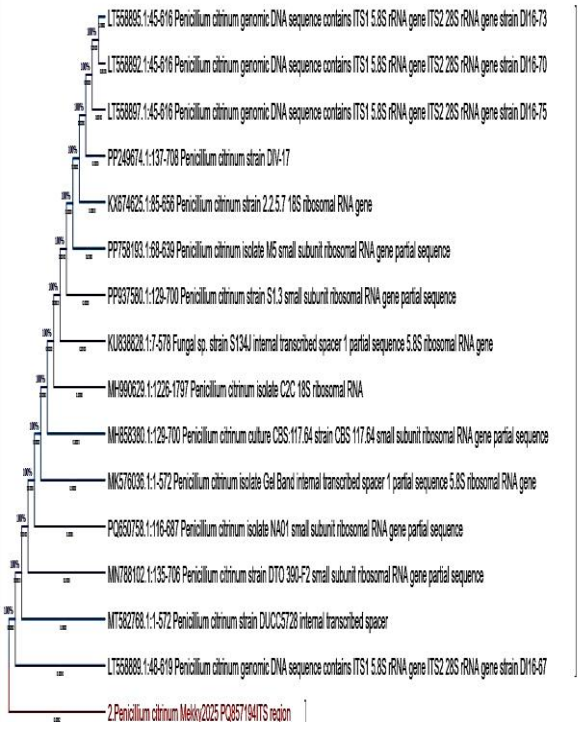

Fig. 1B. Phylogenetic tree for the identified fungus.

GC-Mass testing of PCE

An eleven various bioactive molecules could be seen upon testing *P. citrinum* extract which were Z,Z,Z-4,6,9-Nonadecatriene; butanoic acid, 3,7-dimethyl-2,6-octadienyl ester, (E); 1,3,7 Octatriene, 3,7-dimethyl-, (E)-; 1,6-Octadien-3-ol, 3,7-dimethyl; Nerolidol-epoxyacetate; n-Hexadecanoic acid; 9-Octadecenoic acid (Z)-; [1,1'-Bicyclopropyl]-2- Octadecatrienoic acid, 2'-hexyl-, methyl ester; 9,12,15-Octadecatrienoic acid, 2,3-dihydroxypropyl ester, (z,z,z)-; 9,12-Octadecadienoic acid (z,z)- and Isosolanidine.

It could be noticed that: 9,12-Octadecadienoic acid (z,z)- and n-Hexadecanoic acid were the most common compound in the extract subsequently as shown in (Fig. 2 and Table. 1).

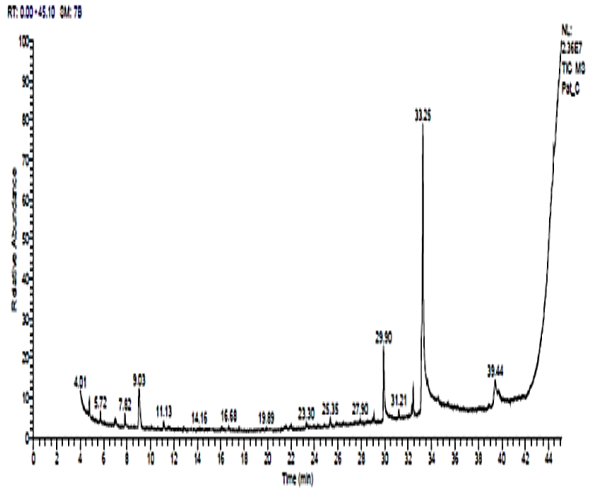

Fig.2. GC-Mass chromatogram illustrating different compounds in PCE.

Characterization for ZnO-NPs

The produced ZnO-NPs showed a white color with a distinctive peak of 363 nm upon examination using UV spectrophotometer with a particle size of 85±4.6 nm upon TEM examination (Fig. 3D and 3E). FTIR pattern showed a peak at 350 cm^{-1} in ZnO-NPs, and another peak at 1558 cm^{-1}, which assigned to O-H bending. However, the peak that could be seen 111.98 cm^{-1} for carbonyl stretching for ZnO-NPs. Also, the broad absorption peak of 3320 cm^{-1} can be attributed to the characteristic absorption of hydroxyl group. Furthermore, a band at 2926 and a peak at 1558 cm^{-1} come from the stretching and bending of C-H, subsequently as seen in (Fig. 3F). Additionally, XRD analysis revealed the shape of the zinc oxide at angels for 2[Theta] at (100, 101, 103, 105, 103 as seen in (Fig. 4A).

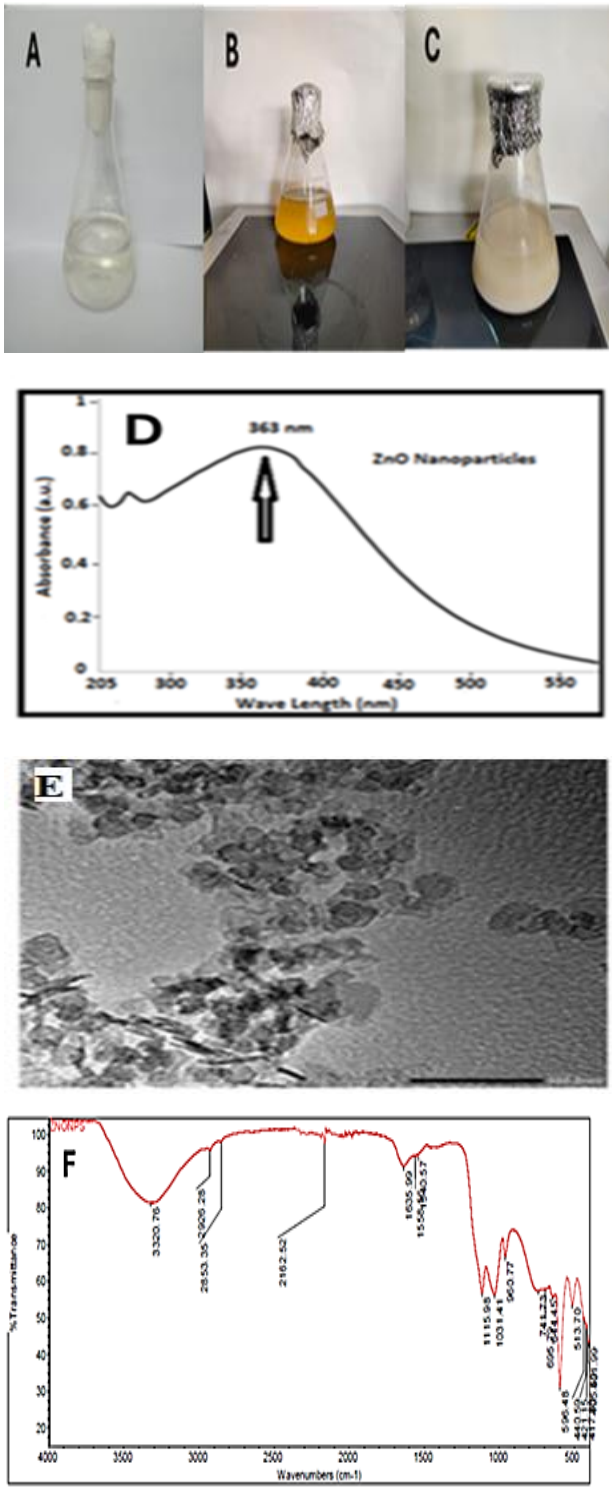

Fig. 3. Production and characterization of ZnO-NPs: (A) Zn $(NO_3)_2.6H_2O$ as precursor, (B) Fungal filtrate, (C) Synthesized ZnO-NPs showing visible color change, (D) UV–Visible absorption spectrum of ZnO-NPs showing the surface plasmon resonance (SPR) peak, (E) TEM image showing the morphology and size distribution of the ZnO-NPs, and (F) FTIR spectrum confirming the functional groups involved in ZnO-NP stabilization.

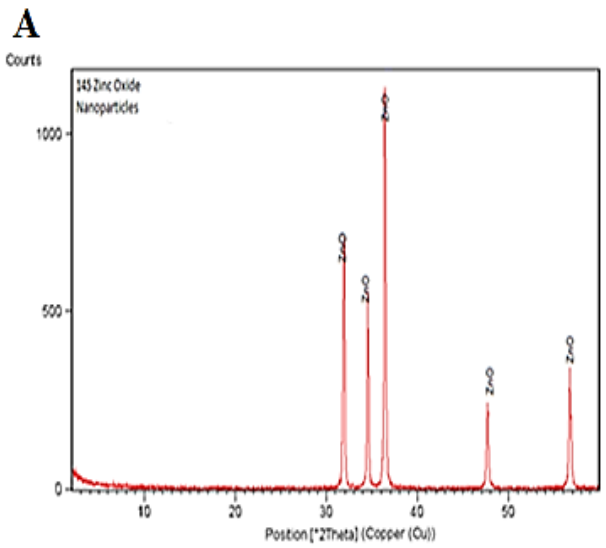

Fig. 4. X-ray diffraction analysis of ZnO-NPs

Antifungal assay for ZnO nanoparticles and PCE

The prepared fungal extract as well as the ZnO NPs were tested versus: *Aspergillus fumigates* (ATCC46645), *Candida albicans* (ATCC6538), *C. krusei* (ATCC32196), and *C. parasilosis* (ATCC22019). The produced ZnO nanoparticles showed the highest antifungal impact versus *C. albicans*, and its minimal inhibitory levels were determined with a value of 125±0.4 µg/ml followed by the fungal extract antifungal impact versus *C. albicans* and its minimal inhibitory levels was determined with a value of 250± 0.4 µg/ml (Fig. 5 and Table 2)

Table 1. GC–MS analysis showing the chemical constituents identified in the PCE.

RT	Compound	Peak Area (%)	Chemical formula	Molecular Weight (g/mol)
4.77	Z,Z,Z-4,6,9-Nonadecatriene	2.22	$C_{19}H_{34}$	260
5.72	Butanoic acid, 3,7-dimethyl-2,6-octadienyl ester, (E)	1.85	$C_{14}H_{24}O_2$	224
7.82	1,3,7-Octatriene, 3,7-dimethyl-, (E)-	2.02	$C_{10}H_{16}$	136
9.02	1,6-Octadien-3-ol, 3,7-dimethyl	8.94	$C_{10}H_{18}O$	154
25..35	Nerolidol-epoxyacetate	1.69	$C_{17}H_{28}O_4$	296
29.90	n-Hexadecanoic acid	13.34	$C_{16}H_{32}O_2$	256
31.21	9-Octadecenoic acid (Z)-	1.52	$C18H_{34}O_2$	282
32.3	[1,1'-Bicyclopropyl]-2- Octadecatrienoic acid, 2'-hexyl-, methyl ester	1.44	$C21H38O_2$	322
32.43	9,12,15-Octadecatrienoic acid, 2,3-dihydroxypropyl ester, (z,z,z)-	4.03	$C_{21}H_{36}O_4$	352
33.25	9,12-Octadecadienoic acid (z,z)-	57.27	$C18H_{32}O_2$	280
39.43	Isosolanidine	5.68	$C_{27}H_{43}NO$	397

Where, RT; is Retention tim

Table 2. Antifungal impact (Cm) of extract of *P. citrinum* and the produced ZnO-NPs versus different fungal isolates (Outcomes were recoded as means ± SD).

Strains	**PCE**	**ZnO-NPS**	**Antifungal drug**
A. fumigates (ATCC46645)	1.2±0.2	1.4±0.1	1.8±0.2
C. albicans (ATCC6538)	2.0±0.1	2.3±0.2	2.1±0.2
C. krusei (ATCC32196)	1.6±0.2	1.7±0.2	1.9±0.3
C. parasilosis (ATCC22019)	1.7±0.1	1.8±0.2	2.3±0.2

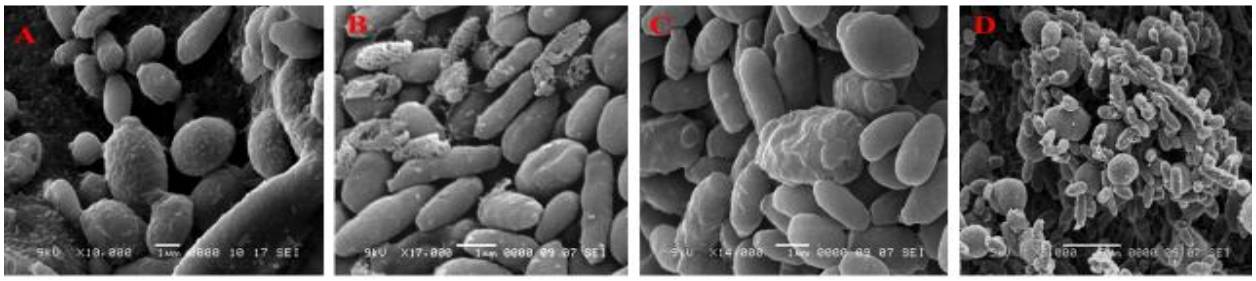

Fig. 6. SEM for *C. albicans* (A) Untreated; (B) Treated by PCE; (C) Treated by ZnO-NPs; (D) Treated by standard antifungal drug(Magnification= 17000 X).

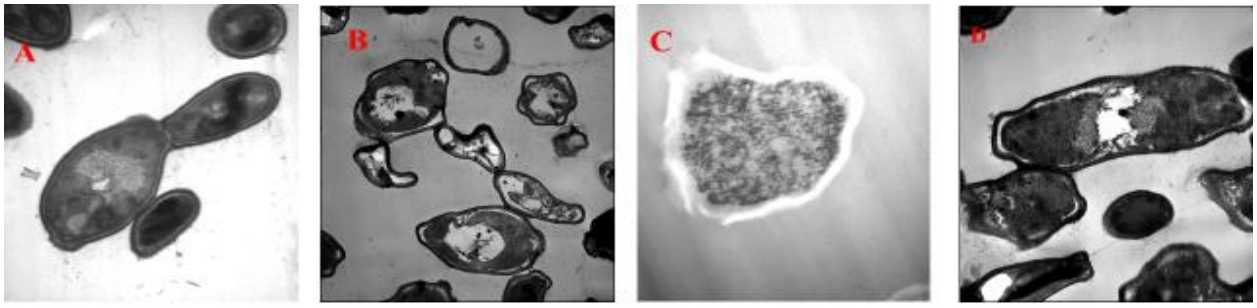

Fig. 7. TEM for *C. albicans* (A) Untreated; (B) Treated by PCE; (C) Treated by ZnO-NPs; (D) Treated by standard antifungal drug (Magnification= 10000 X).

Antioxidant values of various treatments

The antioxidant outcome of ascorbic acid as a standard was evaluated and showed a value of IC_{50} =2.71±0.6 µg/ml, while the antioxidant outcome for the fungal extract was detected with the antioxidant level at IC_{50}= 8.78 ±0.4 µg/ml. Besides, ZnO-NPs had an antioxidant level at IC_{50}= 5.41 ±0.3 µg/ml (Fig. 8).

Hemolytic activities of various treatments

The hemolytic activity of the standard drug indomethacin was observed with an IC_{50} value of 8.02 ± 0.1 µg/mL. In comparison, the biosynthesized ZnO-NPs exhibited a notable anti-inflammatory effect with an IC_{50} of 13.51 ± 0.3 µg/mL. PCE showed a moderate effect, with an IC_{50} value of 19.71 ± 0.6 µg/mL, as illustrated in Fig. 9.

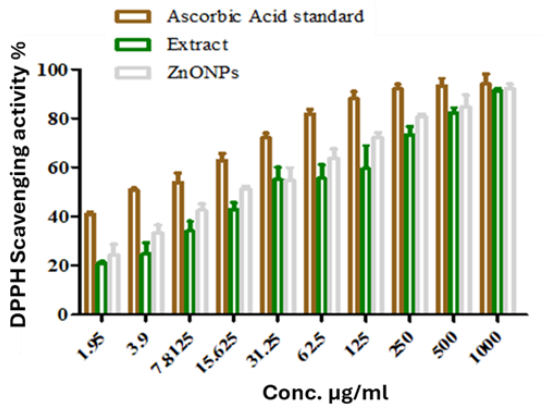

Fig. 8. Antioxidant impact of PCE and the produced ZnO-NPs (Results are reported as means ± SD).

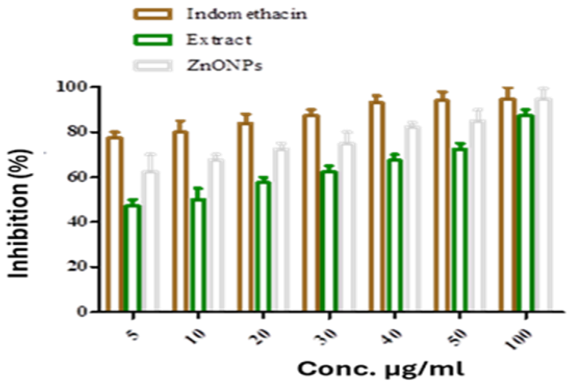

Fig. 9. Hemolytic activities of PCE and the produced ZnO-NPs (Outcomes are represented as means ± SD).

Cytotoxicity of various treatments towards normal cells

Assessment the cytotoxic impact of fungal extract and ZnO-NPS through MTT test showed their potent impact towards normal cells with CC_{50s}=18.2±0.7 and 22.6±0.7 µg/ml, respectively (Fig. 10 A and B).

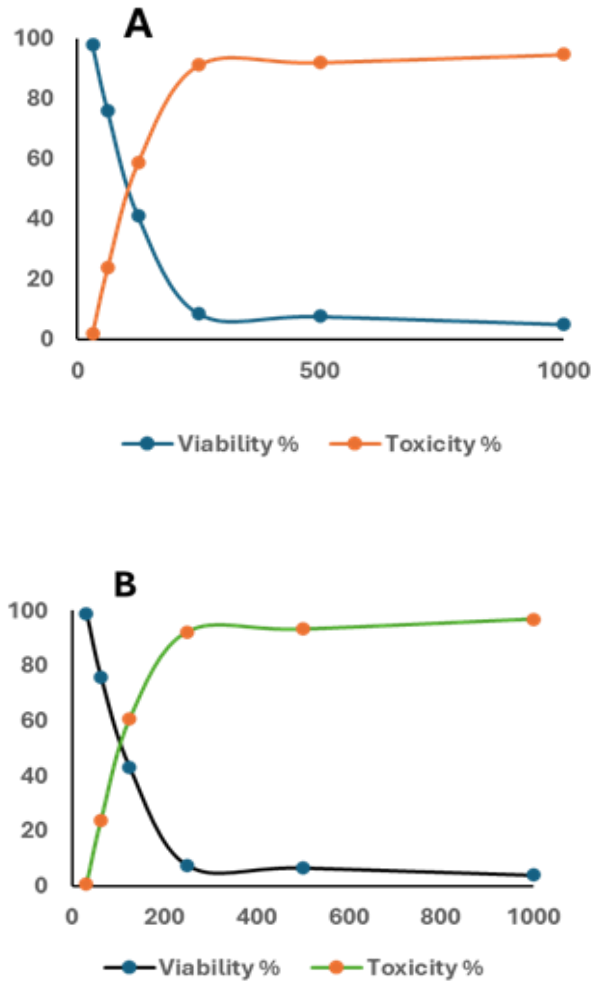

Fig. 10. Cytotoxicity for PCE (A) and the produced ZnO-NPs (B) towards WI-38 normal human lung fibroblast cells (Results are reported as means ± SD).

Discussion

The metal oxide nanoparticles are used in a wide range of applications (Mekky et al., 2021). For green synthesis of such these metal oxide NPs, natural products including fungi have been applied (Saied et al., 2023). Fungal strains are used for reduction of metal and metal oxides to nanostructure, which results in long-term limiting and consolidation of products; therefore, it is advised that green generating NPs employing these strains are used. Additionally, the problems that were caused by the application of mechanical and chemical processes are resolved by the development of NPs using these methods of production (Abd-Elhameed et al., 2024). Fungi are preferred over other microbes because they are easy to manage, produce a significant quantity of biomass, produce a lot of extrinsic chemicals, collect resistant components, and are easy to grow (Mohammed et al., 2024). In order to produce ZnO-NPs, the current study investigated how well the isolated fungus reduced, capped, and stabilized the metallic oxide material. FN.6 was selected from among the numerous isolated fungal strains based on the intensity of its color, and it was identified as *P. citrinum* through the microscope, culture, and genetic examination. The fungal extract contained a variety of bioactive compounds upon testing using GC-Mass analysis. The family of metal oxides, which includes ZnO-NPs, is distinguished by its ability to photocatalyze and photooxidize biological and chemical molecules (Sharma et al., 2010). Cotton textiles were also used to create persistent nanoparticles (Hussein et al., 2018). The compounds that *P. citrinum* FN.6 produced, such as proteins, and amino acids. When the microbiological filtrate combined with metal, its color turned to whitish, which was the first indication that ZnO-NPs were being produced. As previously mentioned, the deep color indicates the complete reduction of all Zn ions to ZnO. Amino acids were used as reducing agents to create nanoscale structure in metal precursors, and the final product was capped and stabilized. The intensity of the color is associated with the proportions that decrease metallic ions via fungal products (El-Naggar et al., 2017). The XRD results obtained for ZnO-NPs' eco-friendly procedures are in line with earlier studies (Agarwal et al., 2017). The peak structure of scattering at 2θ ratios that vary from 35° − 60° demonstrate the process by which fungal molecules create ZnO-NPs (Dobrucka et al., 2018). According to XRD analysis, the unique structure seen and the absence of additional diffraction peak frequencies indicate that the produced ZnO-NPs were uniform (Sánchez-Pérez et al., 2023).

In this study both PCE and the produced ZnO-NPs were tested versus various fungal pathogens where both of them showed the highest activity towards *C. albicans* and the alterations for the cellular organelles were examined using both types of electron microscopy including TEM and SEM. In accordance with (Singh et al., 2018) who illustrated the antimicrobial action of ZnO-NPs. Examining the antioxidant potential of NPs that will be introduced into biological structures is an essential step. Free radicals are produced in a variety of biological procedures by the interaction of oxygen molecules with macromolecules (Consolo et al., 2020; Alshawwa et al., 2022). Having many unpaired electrons, these radicals are very unstable and damage cells by passing electrons across them to stabilize them. The antioxidant qualities of both synthetic and natural materials have been connected to a number of processes, such as peroxide decomposition, chain-initiating prevention, molecular oxygen acquisition prevention, reactive oxygen species rescue, and lowering capability (Bahrulolum et al., 2021). This study reported that ZnO-NPs had the highest antioxidant level

The hemolytic assay revealed a marked reduction in red blood cell lysis following treatment with biosynthesized ZnO-NPs, suggesting their protective effect against membrane destabilization (Salem et al., 2021). This behavior is likely due to the structural integrity and favorable surface chemistry of the nanoparticles, which may interact with erythrocyte membranes in a non-disruptive manner, preserving their morphology and function (Khan et al., 2025). In contrast to chemically synthesized compounds that may induce oxidative stress and trigger hemolysis, green-synthesized ZnO-NPs are capped with biologically active moieties that enhance biocompatibility. The presence of antioxidant phytochemicals and fatty acid derivatives on the nanoparticle surface contributes to phospholipid bilayer stabilization, minimizing osmotic imbalance and cellular rupture (Shah et al., 2025).

Comparative studies with the crude fungal extract revealed a relatively weaker anti-hemolytic effect, suggesting that nanoparticle formulation improves the bioactivity of the native constituents (Tuorkey et al., 2022). These findings align with previous reports on green nanomaterials that exert protective effects on blood cells, supporting their potential use in biomedical applications requiring hemocompatibility. Moreover, Salem et al. (2021) reported that ZnO-NPs synthesized via plant extracts and gamma irradiation not only possessed strong antibacterial properties but also significantly inhibited red blood cell hemolysis in the presence of multidrug-resistant pathogens. The enhanced hemocompatibility in their study was attributed to the synergistic effect of phytochemical capping agents and precise control over particle features.

Additionally, Khan et al. (2025) showed that the synthesis method substantially influences hemolytic activity. Their results demonstrated that ZnO and ZnS nanoparticles synthesized via wet chemical routes induced variable levels of red blood cell lysis, particularly at higher doses. In contrast, the biosynthesized ZnO-NPs in our study showed markedly lower hemolytic activity, likely due to the stabilizing effect of fungal-derived surface biomolecules.

The MTT test method is sensitive, accurate, colorimetric, and capable of evaluating biochemical cell functions by measuring living cells after active substances are administered (Shkir et al., 2020). The effectiveness of fungal-mediated ZnO-NPs in comparison to the normal cell line (Wi-38) was investigated utilizing the MTT measurement technique. The obtained results are in line with those reported by (Fouda et al., 2018), who discovered that the quantity of green generated ZnO-NPs administered had no effect on the lifetime of normal cell lines at different concentrations.

Conclusion

The fungal isolate, identified as *P. citrinum* FN.6 by both traditional approaches and molecular verification, was successfully used in this investigation to synthesize ZnO-NPs.

Fatty acids were the most prevalent components in the fungal extract, which contains a wide range of chemicals. The synthesized ZnO-NPs exhibited peak SPR at a wavenumber of 363 nm, demonstrating ZnO-NPs' SPR. Additionally, the shapes and structural architectures of the produced nanoparticles were identified using TEM and XRD. The DPPH approach, which shows the scavenging capability, was used to evaluate the reduction potential of ZnO-NPs. Its outstanding hemolytic activities were demonstrated by membrane stabilization test. Furthermore, ZnO-NPs exhibited minimal detrimental effects to normal healthy cells.

5. Reference

Aamer HA, Elalem SF, Al-Askar AA, Sharaf OA, Gaber MA, Kowalczewski P, Behiry S, Abdelkhalek A, 2024. Antioxidant and antimicrobial activities of *Salsola imbricata* methanolic extract and its phytochemical characterization. Open Life Sci.19:20221011.

Abd-Elhameed AY, Eladly AM, Abdel-radi AW, Mekky AE, 2024. In vitro Myco-Synthesized copper oxide nanoparticles: a promising antiviral agent with antioxidant, anti-inflammatory, and anti-cancer activity. Microb. Biosyst. 9: 2024.317736

Abozaid IA, Mahdy HM, Haroun SA, Mekky A E, 2024. Aspergillus terreus Mekky221, as a potential candidate fungus for biodiesel production using sugar cane bagasse and rice straw as inexpensive carbon sources. Microbial Biosystems. 9:133-142.

Agarwal H, Kumar SV, Rajeshkumar S, 2017. A review on green synthesis of zinc oxide nanoparticles—an eco-friendly approach. Resour-Eff Technol. 3, Issue 4: 406-413.

Alavi M, Nokhodchi A, 2021. Synthesis and Modification of Bio-Derived Antibacterial Ag and ZnO Nanoparticles by Plants, Fungi, and Bacteria. Drug Discov. Today. 26: 1953–1962.

Alshawwa SZ, Mohammed EJ, Hashim N, Sharaf M, Selim S, Alhuthali HM, Alzahrani HA, Mekky AE, Elharrif MG, 2022. In Situ Biosynthesis of Reduced Alpha Hematite (α-Fe2O3) Nanoparticles by Stevia Rebaudiana L. Leaf Extract: Insights into Antioxidant, Antimicrobial, and Anticancer Properties. Antibiotics. 11: 1252.

Anand A, Nussana L, Sham Aan MP, Ekwipoo K, Sangashetty SG, Jobish J, 2020. Synthesis and characterization of ZnO nanoparticles and their natural rubber composites. J. Macromol. Sci. 59:697-712.

Ayub H, Jabeen U, Ahmad I, Aamir M, Ullah A, Mushtaq A, Behlil F, Javaid B, Syed A, Elgorban AM, Bahkali AH, Zairov R, Ali A, A, 2024. Enhanced anticancer and biological activities of environmentally friendly Ni/Cu-ZnO solid solution nanoparticles. Heliyon.10(23): e39912.

Bahrulolum H, Nooraei S, Javanshir N, Tarrahimofrad H, Mirbagheri VS, Easton AJ, Ahmadian G, 2021. Green synthesis of metal nanoparticles using microorganisms and their application in the agrifood sector. J Nanobiotechnol. 19:86.

Moghaddam BA, Namvar F, Moniri M, Md Tahir P, Azizi S, Mohamad R, 2015. Nanoparticles Biosynthesized by Fungi and Yeast: A Review of Their Preparation, Properties, and Medical Applications. Molecules.20(9):16540-65.

Carrouel F, Viennot S, Ottolenghi L, Gaillard C, Bourgeois D, 2020. Nanoparticles as Anti-microbial, Anti-inflammatory, and Remineralizing Agents in Oral Care Cosmetics: a Review of the Current Situation. Nanomaterials. 10 (1): 140.

Consolo VF, Torres-Nicolini A, Alvarez VA, 2020. Mycosinthetized Ag, CuO and ZnO nanoparticles from a promising *Trichoderma harzianum* strain and their antifungal potential against important phytopathogens. Sci Rep.10:20499.

Correa LO, Bezerra AFM, Honorato LRS, Cortez ACA, Souza JVB, Souza ES, 2021. Amazonian soil fungi are efficient degraders of glyphosate herbicide; novel isolates of Penicillium, Aspergillus, and Trichoderma. Braz. J. Biol.83: e242830.

da Silva, BL, Abuçafy MP, Manaia EB, Junior JAO, Chiari-Andréo BG, Pietro RCR, Chiavacci LA, 2019. Relationship between Structure and Antimicrobial Activity of Zinc Oxide Nanoparticles: An Overview. Int. J. Nanomed. 14: 9395–9410.

Sharma D, Rajput J, Kaith BS, Kaur M, Sharma S, 2010. Synthesis of ZnO nanoparticals and study of their antibacterial and antifungal properties. Thin Solid Films 519:1224–1229.

Deleanu IM, Busuioc C, Deleanu M, Stoica-Guzun A, Rotaru M, Ștefan VA, Isopencu G, 2024. Antimicrobial Carboxymethyl Cellulose-Bacterial Cellulose Composites Loaded with Green Synthesized ZnO and Ag Nanoparticles for Food Packaging. Int. J. Mol. Sci.25:12890.

Dobrucka R, Dlugaszewska J, Kaczmarek M, 2018. Cytotoxic and antimicrobial effects of biosynthesized ZnO nanoparticles using of *Chelidonium majus* extract. Biomed. Microdevices. 20:5

Eixenberger JE, Anders CB, Hermann RJ, Brown RJ, Reddy KM, Punnoose A, Wingett DG, 2017. Rapid Dissolution of ZnO Nanoparticles Induced by Biological Buffers Significantly Impacts Cytotoxicity. Chem. Res. Toxicol. 30: 1641–1651.

El-Naggar ME, Shaarawy S, Hebeish AA, 2017. Multifunctional properties of cotton fabrics coated with in situ synthesis of Zinc oxide nanoparticles capped with date seed extract. Carbohydr Polym. 181:307-316.

Fouda A, Hassan SED, Salem SS, Shaheen TI, 2018. In-Vitro cytotoxicity, antibacterial, and UV protection properties of the biosynthesized Zinc oxide nanoparticles for medical textile applications. Microb. Pathog. 125: 252–261.

Hefny ME, El-Zamek FI, El-Fattah HIA, Mahgoub SA, 2019. Biosynthesis of Zinc Nanoparticles Using Culture Filtrates of Aspergillus, Fusarium and Penicillium Fungal Species and Their Antibacterial Properties against Gram-Positive and Gram-Negative Bacteria. Zagazig J. Agric. Res. 46: 2009–2021.

Hussein J, El-Banna M, Razik TA, El-Nagga ME, 2018. Biocompatible zinc oxide nanocrystals stabilized via hydroxyethyl cellulose for mitigation of diabetic complications. Int. J. Biol. Macromol. 107:748-754.

Jain KK, 2007. Applications of nanobiotechnology in clinical diagnostics. Clin. Chem. 53:2002–2009.

Jiang Q, Kang Z, Wang X, Zhao C, 2024. Molecular phylogeny and morphology reveal three new plant pathogenic fungi species (Septobasidiales, Basidiomycota) from China. MycoKeys.111:229-248.

Khan, T.F., Muhyuddin, M., Irum, S., Ali, M.A., Husain, S.W. and Basit, M.A., 2025. Comparing the antioxidant and hemolytic activity of wet-chemically synthesized ZnO, ZnS, and ZnO/ZnS nanocomposite. *Inorganic Chemistry Communications*, *174*, p.113902.

Liu J, Qiao SZ, Hu QH, 2011. Magnetic nanocomposites with mesoporous structures: Synthesis and applications. Small 7:425–443.

Luna-Vázquez-Gómez, R., Arellano-García, M.E., García-Ramos, J.C., Radilla-Chávez, P., Salas-Vargas, D.S., Casillas-Figueroa, F., Ruiz-Ruiz, B., Bogdanchikova, N. and Pestryakov, A., 2021. Hemolysis of human erythrocytes by Argovit™ AgNPs from healthy and diabetic donors: An in vitro study. Materials, 14(11), p.2792.

Maťátková O, Michailidu J, Miškovská A, Kolouchová I, Masák J, Čejková A, 2022. Antimicrobial Properties and Applications of Metal Nanoparticles Biosynthesized by Green Methods. Biotechnol. Adv.58: 107905.

Mekky AE, Farrag AA, Hmed AA, Sofy A, 2021. Preparation of zinc oxide nanoparticles using *Aspergillus niger* as antimicrobial and anticancer agents. J. Pure Appl. Microbiol. 15: 1547-1566.

Mekky, A.E., Abdelaziz, A.E., Youssef, F.S., Elaskary, S.A., Shoun, A.A., Alwaleed, E.A., Gaber, M.A., Al-Askar, A.A., Alsamman, A.M., Yousef, A. and AbdElgayed, G., 2024. Unravelling the Antimicrobial, Antibiofilm, Suppressing Fibronectin Binding Protein A (fnba) and cna Virulence Genes, Anti-Inflammatory and Antioxidant Potential of Biosynthesized Solanum lycopersicum Silver Nanoparticles. Medicina, 60(3), p.515.

Mohammed EJ, Abdelaziz AE, Mekky AE, Mahmoud NN, Sharaf M, Al-Habibi MM, Shoun AA, 2024. Biomedical Promise of *Aspergillus flavus*-Biosynthesized Selenium Nanoparticles: A Green Synthesis Approach to Antiviral, Anticancer, Anti-Biofilm, and AntibacterialApplications. Pharmaceuticals.1 7:915.

Mohanpuria P, Rana NK, Yadav SK, 2008. Biosynthesis of nanoparticles: Technological concepts and future applications. J. Nanopart. Res. 10:507–517.

Muhammad W, Ullah N, Haroon M, Abbasi BH, 2019. Optical, Morphological and Biological Analysis of Zinc Oxide Nanoparticles (ZnO Nps) Using *Papaver somniferum* L. RSC Adv. 9: 29541–29548.

Naveed M, Ali I, Aziz T, Saleem A, Rajpoot Z, Khaleel S, Khan AA, Al-Harbi M, Albekairi TH, 2025 Computational and GC-MS screening of bioactive compounds from *Thymus Vulgaris* targeting mycolactone

protein associated with Buruli ulcer. Sci Rep.15(1):131.

Pesaresi M, Pirani F, Tagliabracci A, Valsecchi M, Procopio AD, Busardò FP, 2020. SARS-CoV-2 identification in lungs, heart and kidney specimens by transmission and scanning electron microscopy. Eur. Rev. Med. Pharmacol. Sci. 24:5186–5188.

Prabha RK, Jajoo A, 2021. Priming with Zinc Oxide Nanoparticles Improve Germination and Photosynthetic Performance in Wheat. Plant Physiol. Biochem.160: 341–351.

Pragati J, Poonam K, Rana JS, 2018. Green synthesis of zinc oxide nanoparticles using flower extract of *Nyctanthes arborists* and their 42al activity. J. King Saud Univ. Sci. 30:168–175.

Reza MZ, Oppong-Danquah E, Tasdemir D, 2024. The Impact of the Culture Regime on the Metabolome and Anti-Phytopathogenic Activity of Marine Fungal Co-Cultures. Mar Drugs.22:66.

Al-Zahrani SS, Al-Garni MS. Antifungal potentiality of mycogenic silver nanoparticles capped with chitosan produced by endophytic *Amesia atrobrunnea*. Saudi J Biol Sci. 30:103746.

Saied E, Mekky AE, Al-Askar AA, Hagag AF, El-bana AA, Ashraf M, Walid A, Nour T, Fawzi MM, Arishi AA, Hashem AH, 2023. *Aspergillus terreus*-Mediated Selenium Nanoparticles and Their Antimicrobial and Photocatalytic Activities. Crystals.13:450.

Sánchez-Pérez DM, Flores-Loyola E, Márquez-Guerrero SY, Galindo-Guzman M, Marszalek JE, 2023. Green Synthesis and Characterization of Zinc Oxide Nanoparticles Using *Larrea tridentata* Extract and Their Impact on the In-Vitro Germination and Seedling Growth of *Capsicum annuum*. Sustainability. 15: 3080.

Salem, M.S.E.D., Mahfouz, A.Y. and Fathy, R.M., 2021. The antibacterial and antihemolytic activities assessment of zinc oxide nanoparticles synthesized using plant extracts and gamma irradiation against the uro-pathogenic multidrug resistant Proteus vulgaris. *Biometals*, *34*, pp.175-196.

Sayed R, Safwat NA, Amin BH, Yosri M, 2022. Study of the dual biological impacts of aqueous extracts of normal and gamma-irradiated *Galleria mellonella* larvae. J Taibah Univ Med Sci.17:765-773.

Shkir M, Chandekar KV, Alshehri BM, Khan A, AlFaify S, Hamdy MS, 2020. A remarkable enhancement in photocatalytic activity of facilely synthesized Terbium@Zinc oxide nanoparticles. Appl. Nanosci. 10: 1811–1823.

Shah, S., Chauhan, H., Madhu, H., Mori, D., Soniwala, M., Singh, S. and Prajapati, B., 2025. Lipids fortified nano phytopharmaceuticals: a breakthrough approach in delivering bio-actives for improved therapeutic efficacy. *Pharmaceutical Nanotechnology*, *13*(1), pp.70-89.

Shobha N, Nanda N, Giresha S, 2019. Synthesis and characterization of zinc oxide nanoparticles utilizing seed source of *Ricinus communis* and studying its antioxidant, antifungal, and anticancer activity. Mat Sci. Eng. C. 97:842–850.

Singh AK, Pal P, Gupta V, Yadav TP, Gupta V, Singh SP, 2018. Green synthesis, characterization and antimicrobial activity of zinc oxide quantum dots using *Eclipta alba*. *Mater.* Chem. Phys. 203: 40–48

Sirelkhatim A, Mahmud S, Seeni A, Kaus NHM, Ann LC, Bakhori SKM, Hasan H, Mohamad D, 2015. Review on Zinc Oxide Nanoparticles: Antibacterial Activity and Toxicity Mechanism. Nanomicro Lett. 7:219-242.

Sumanth B, Lakshmeesha TR, Ansari MA, Alzohairy MA, Udayashankar AC, Shobha B., Niranjana SR, Srinivas C, Almatroudi A, 2020. Mycogenic Synthesis of Extracellular Zinc Oxide Nanoparticles from *Xylaria acuta* and Its Nanoantibiotic Potential. Int. J. Nanomedicine.15:8519-8536.

Teodori L, Tagliaferri F, Stipa F, Valente MG, Coletti D, Manganelli A, 2000. Selection, establishment and characterization of cell lines derived from a chemically-induced rat mammary heterogeneous tumor, by flow cytometry, transmission electron microscopy, and immunohistochemistry. In Vitro Cell Dev Biol Anim.; 36:153–162.

Tuorkey, M., Khedr, Y., Aborhyem, S. and Xue, X., 2022. Green synthesis of chicory (Cichorium intybus L.) Chitosan nanoparticles and evaluation of their anti-fungal, anti-hemolytic, and anti-cancer activities. *Journal of Bioactive and Compatible Polymers*, *37*(6), pp.421-436.

Wang X, Ahmad M, Sun H, 2017. Three-Dimensional ZnO Hierarchical

Nanostructures: Solution Phase Synthesis and Applications. Materials.10: 1304.

Wiesmann N, Tremel W, Brieger J, 2020. Zinc Oxide Nanoparticles for Therapeutic Purposes in Cancer Medicine. J. Mat. Chem. B. 8 (23): 4973–4989.

Wojnarowicz J, Chudoba T, Koltsov I, Gierlotka S, Dworakowska S, Lojkowski W, 2018. Size Control Mechanism of ZnO Nanoparticles Obtained in Microwave Solvothermal Synthesis. Nanotechnology. 29: 065601.

Allawi YM, Al-Taie SB, Hmoshi RM, 2022. Isolation and Identification of *Penicillium rubens* from the Local Strain in Mosul, Iraq, and Investigation of Potassium Phosphate Effect on its Growth. Arch. Razi. Inst.77:421-427.

Yusof HM, Mohamad R, Zaidan UH, Rahman NAA, 2019. Microbial Synthesis of Zinc Oxide Nanoparticles and Their Potential Application as an Antimicrobial Agent and a Feed Supplement in Animal Industry: A Review. J. Anim. Sci. Biotechnol. 10: 57.

Yuvakkumar R, Suresh J, Joseph NA, Sundararajan M, Hong SI, 2014. Novel green synthetic strategy to prepare ZnO nanocrystals using rambutan (*Nephelium lappaceum* L.) Peel extract and its antibacterial applications. Mater Sci Eng C. 41:17–27.